Reprinted from *J. Mol. Biol.* (1981) **146**, 143–156

Conformational and Geometrical Properties of β-Sheets in Proteins

III. Isotropically Stressed Configurations

F. R. Salemme

J. Mol. Biol. (1981) **146**, 143–156

Conformational and Geometrical Properties of β-Sheets in Proteins

III. Isotropically Stressed Configurations

F. R. SALEMME

Department of Biochemistry, New Chemistry Building
University of Arizona, Tucson, Ariz. 85721, U.S.A.

(Received 9 October 1979, and in revised form 17 September 1980)

This paper summarizes and contrasts the geometrical and conformational properties of parallel and antiparallel β-sheets. In either case, it is demonstrated that the geometrical surfaces formed by these structures correspond to isotropically stressed configurations. The attainment of such surfaces in protein β-sheets reflects the interaction of the local conformational forces, which induce the individual chains to twist, and the geometrical requirements for interchain hydrogen bonding, which generally tend to resist the introduction of twist into the sheets. Nevertheless, the conformational behavior associated with optimal, interchain hydrogen bond preservation differs for parallel and antiparallel sheet arrangements. It is shown here how these differences, in concert with the forces that introduce stress into the sheet, reflect themselves in the attainment of different isotropically stressed surface configurations in these structures.

1. Introduction

The investigation of the structural properties of twisted β-sheets (Salemme & Weatherford, 1981*a*,*b*) has shown that their crystallographically observed geometrical behavior can be approximated by a generalized model system that assumes the following physical properties. (1) The driving force for sheet twisting has its origin in the slight energetic preference for extended polypeptide chain conformations with local left-handed twist (Ramachandran, 1974). (2) The twisted conformations of β-sheets are those associated with the optimal preservation of the interchain hydrogen bonds, insofar as is consistent with the low-energy geometrical degrees of freedom both within and between the polypeptide chains. (3) Any deformations induced during sheet twisting will reflect themselves in the low energy and slowly varying degrees of freedom within the structure as a whole; i.e. in the backbone torsional angles ϕ, ψ and the low-energy geometrical deformations of the interchain hydrogen bonds. (4) The final configuration of the sheet will be that which distributes any twist-induced stresses most uniformly throughout the sheet as a whole. Since flat β-sheets are highly symmetric structures, this implies that their most uniformly and locally equivalently stressed twisted conformations will be those best preserving the local symmetry of the corresponding flat structure,

0022-2836/81/050143-14 $02.00/0

insofar as is consistent with the geometrical requirements for optimal preservation of the interchain hydrogen bonds.

The objectives of the present work are to (1) demonstrate that the observed β-sheet spatial configurations approximate those of well-known isotropically stressed surfaces, (2) describe how differences in the conformational behavior of parallel and antiparallel sheets result in the frequent attainment of surfaces of different geometry, and (3) show why the crystallographically observed structures do not possess the conformational regularity characteristic of the idealized, isotropically stressed configurations.

2. Results and Discussion

(a) *β-Sheets are isotropically stressed surfaces*

Figure 1 shows views of twisted parallel and mixed β-sheets that are composed of straight-helical polypeptide chains. Both structures were generated by the least-squares optimization of the adjacent interchain hydrogen bonding as described in the accompanying papers (Salemme & Weatherford, 1981*a*,*b*). Although the

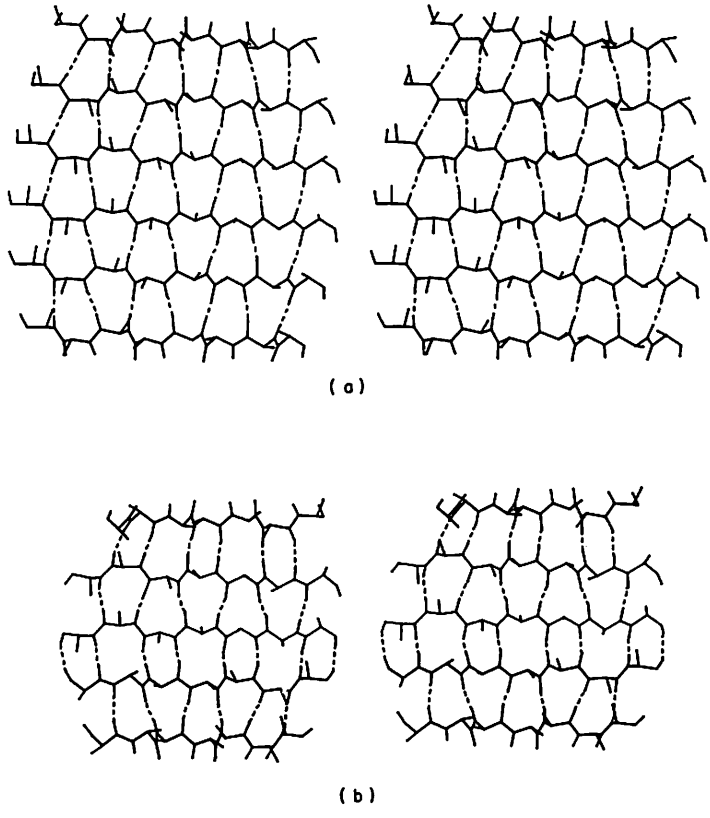

FIG. 1. Extended parallel (a) and mixed (b) β-sheet structures composed of straight-helical polypeptide chains. These structures have the surface geometry of a hyperbolic paraboloid.

hydrogen bonds of these structures become longer toward the ends of the individual chains, it is evident that the overall least-squares optimization of the interchain hydrogen-bonded interactions has symmetrically distributed these distortions so that the structures that result are overall highly symmetric. The surfaces that these structures form are hyperbolic paraboloids (Gellert *et al.*, 1977). This is a well-known isotropically stressed surface configuration that is attained, for example, when a soap film is suspended from a skewed rectangular wire frame (extensive stress), or when a thick (i.e. deformable) sheaf of papers is forced into an envelope that is slightly too small (compressive stress). In the case of rectangular plan β-sheets, the operative forces that give rise to this surface configuration are (1) the minimization of the local polypeptide chain conformational potential that induces the chains to twist (Ramachandran, 1974), and (2) the requirements for interchain hydrogen bonding that tend to resist the introduction of twist into the sheet (see Fig. 4 of Salemme & Weatherford, 1981*a*; Fig. 8 of Salemme & Weatherford,

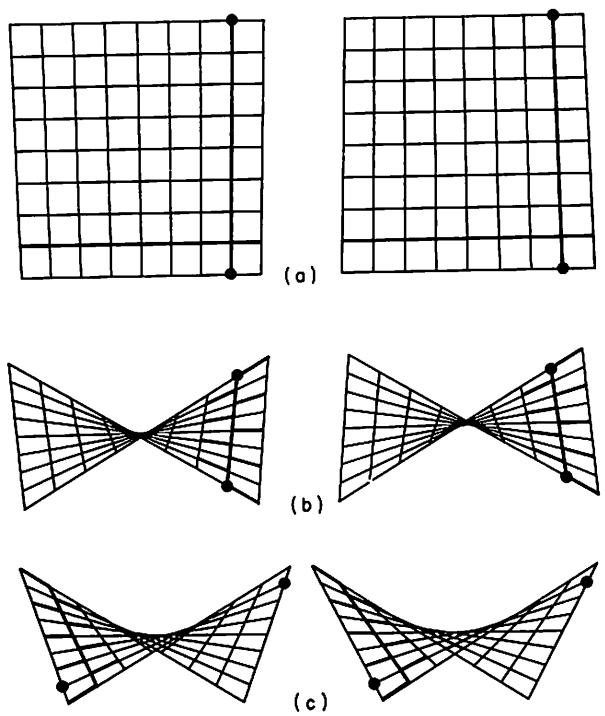

FIG. 2. Stereo views of a hyperbolic paraboloid. The name derives from the fact that vertical cross-sections of maximum curvature are upward- or downward-curved parabolas, while horizontal sections are paired branches of hyperbolas. These are ruled arrays that can be generated from intersecting sets of straight lines, to produce a surface that is locally curved in opposite directions, i.e. anticlastically curved. The formation of such surfaces by twisted β-sheets reflects the twisting tendencies of the polypeptide chains, which behave as a set of helical springs (e.g. unbroken line with dotted endpoints). However, the interchain hydrogen-bonded interactions tend to resist the introduction of twist into the sheet; the extended across-the-sheet interaction effectively corresponding to a set of helical springs that are orthogonal to the polypeptide chains and which resist torsional twist. The equilibration of these opposing forces results in the attainment of an isotropically stressed surface.

1981*b*). In mechanical terms, the surface configuration can be viewed as a result of the equilibration between two locally orthogonal sets of torsional springs (Fig. 2). The first set of these springs lies along the polypeptide chains and introduces twist into the surface. The second set can be viewed to lie along the mean direction of the interchain hydrogen bonds and tends to resist the introduction of twist into the structure. The tendency for rectangular plan β-sheets to form such surfaces when they are located in the interior of proteins, where packing environments are similar on both sides of the sheets, is therefore seen as a natural consequence of the equilibration of the forces within the sheet.

Figure 3 schematically shows a sheet with a staggered polypeptide chain arrangement projected upon a hyperbolic paraboloid surface. It is evident that

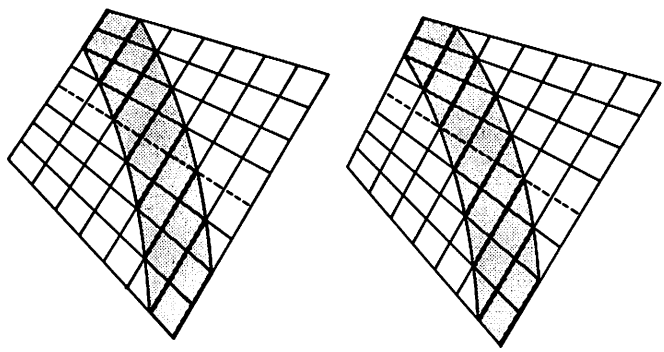

FIG. 3. Schematic view of a β-sheet of staggered plan projected onto a hyperbolic paraboloid. The heavy broken line indicates the line of isotropic stress distribution in the *rectangular* sheet. Truncation of the rectangular sheet wings upsets this balance of forces, so that the stress distribution is no longer uniform in the staggered sheet. As a result, staggered arrays spontaneously deform to surfaces having the geometry of a hyperboloid of one sheet (see Fig. 4).

truncation of the surface to eliminate the sheet wings upsets the balance of forces within the sheet. The isotropically stressed configuration in such a staggered plan sheet is, instead, one in which each chain makes localized, symmetrically stressed interactions with its neighbors (Fig. 4(a) and (b)). As shown previously (Fig. 8 of Salemme & Weatherford, 1981*a*), this results in the formation of a structural configuration of apparent cylindrical symmetry. This surface is, in fact, another doubly curved, isotropically stressed surface (Fig. 4(b) and (c)), which is a catenoid or hyperboloid of one sheet (Gellert *et al.*, 1977). Such surfaces are typically observed when a soap film is suspended between two circular rings.

As first noted by Boys (1959), a catenoid surface formed of a thin, slightly elastic material (such as the plastic used to produce artificial flowers on bent wire frames) may be slit along a radial plane (Fig. 4(c)) and unfolded to produce a helicoid surface (Fig. 4(d)). Since this process corresponds to an isometric deformation of an isotropically stressed surface, this demonstrates that the helical structures shown previously (Fig. 3 of Salemme & Weatherford, 1981*a*; Figs 5 and 11 of Salemme & Weatherford, 1981*b*) are also isotropically stressed surfaces. It is consequently

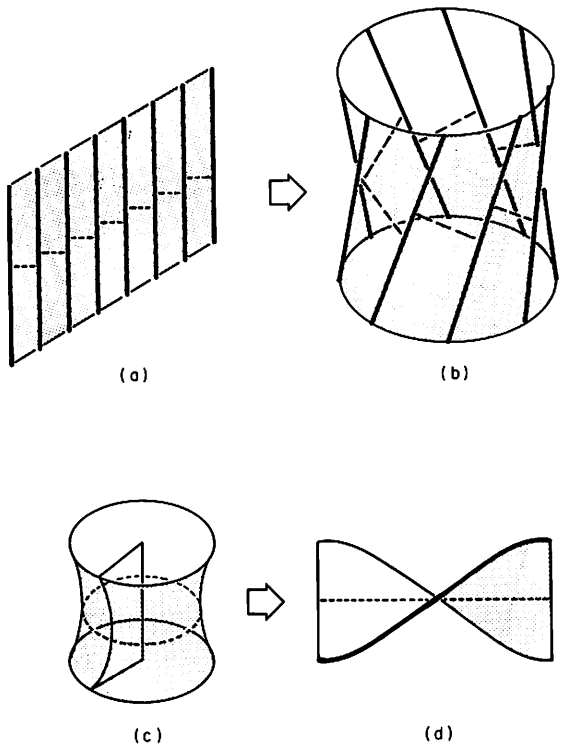

FIG. 4. (a) A plan view of a staggered β-sheet indicating the (broken) lines of symmetrical stress distribution (or interchain closest approach) when the structure is twisted. As shown in (b), twisting results in the formation of a catenoid or hyperboloid of 1 sheet, an anticlastically curved, isotropically stressed surface that results from the combination of interchain twist and rise in the staggered plan sheet. As first noted by Boys (1959), a catenoid surface may be cut along a radial plane (c) and opened to produce a helicoid surface (d).

evident that the majority of observed β-sheet configurations simply reflect a basic stress–strain relationship between the tendency of the individual chains to twist and the tendency of the sheet hydrogen bonding to resist twisting of the sheet as a whole. In what follows, it is described in more detail how the particular geometrical constraints associated with the twisting of parallel and antiparallel β-sheets result in various structural configurations that reflect isotropic stress distribution in the structures.

(b) *Summary properties of protein β-sheets*

Figure 5 summarizes the geometrical properties of protein β-sheets. Figure 5(a) shows the spatial behavior of the parallel coiled-coil, a configuration that optimizes the conflicting requirements of interchain hydrogen bonding and polypeptide chain twist between isolated pairs of polypeptide chains. For the reasons outlined previously (see Fig. 5 of Salemme & Weatherford, 1981*a*), such conformational arrangements are not readily extensible into multiple-strand structures unless they

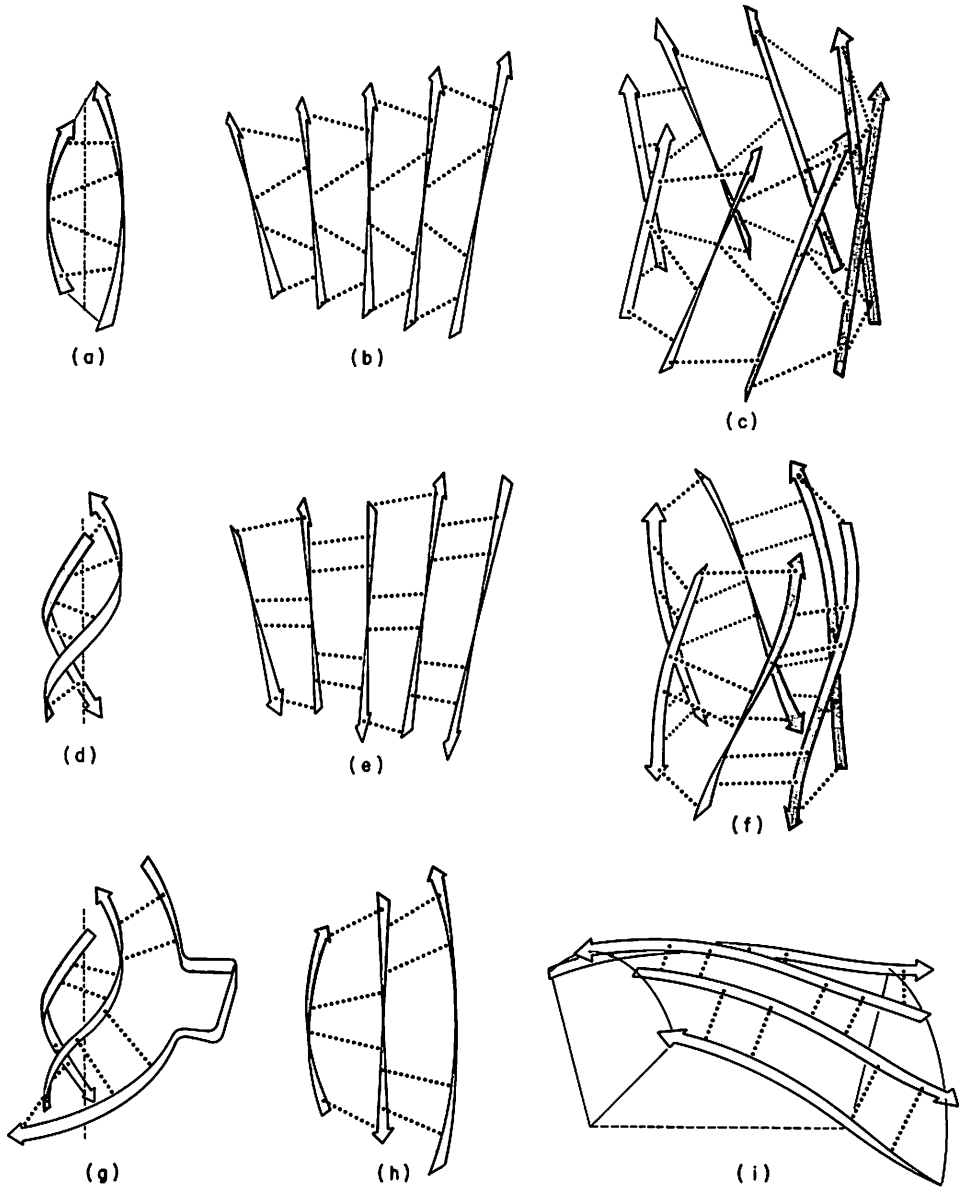

FIG. 5. Schematic illustration of isotropically stressed β-sheets. (a) A parallel coiled-coil. Distorted versions of this arrangement occur principally in β-barrels where they typically effect some extent of local curvature required to close the structure. (b) A parallel hyperbolic paraboloid composed of straight helical crossing chains. (c) A parallel barrel made of a staggered array of straight-helical crossing chains. Observed structures typically have more extensive interchain hydrogen bonding than is compatible with the extensive twisting required for closure, and so incorporate conformational or hydrogen-bonded irregularities and local regions of coiled-coil conformation. (d) An antiparallel coiled-coil that can occur in many variations and can be much more extensively twisted than the parallel double strand coiled-coil. (e) Antiparallel hyperbolic paraboloid. Regular configurations are relatively infrequently observed owing to the conformational flexibility associated with the interchain hydrogen-bond geometry, which allows them to be readily deformed in response to extended packing interactions. (f) An antiparallel

are so slightly twisted as to be practically indistinguishable from conformationally similar straight-helical chains. Further, the fact that isolated parallel double-strand parallel sheets are rarely observed in known proteins (Richardson, 1977) would appear to be related to the observation that highly twisted arrangements that might potentially give rise to the intimate side-chain packing attained in antiparallel coiled-coils (see Fig. 9 of Salemme & Weatherford, 1981*b*) would result in very highly strained parallel structures (see Fig. 4 of Salemme & Weatherford, 1981*a*). Parallel structures, instead, appear to generally provide packing surfaces for α-helices, so giving rise to βαβ packing domains (Richardson, 1976; Sternberg & Thornton, 1976).

Figure 5(b) shows the isotropically stressed arrangement attained in parallel sheets of rectangular plan, the anticlastically curved hyperbolic paraboloid. Owing to conformational restrictions arising from the requirements of interchain hydrogen-bonding geometry, such structures tend to have constant rates of interchain twist (see Fig. 2 of Salemme & Weatherford, 1981*a*), the extent of which is related to the extensiveness of interchain hydrogen bonding both along and across the polypeptide chains (see Fig. 4 of Salemme & Weatherford, 1981*b*).

Figure 5(c) shows an idealized anticlastically curved, isotropically stressed, surface configuration of the parallel staggered-sheet, which is basically that of a catenoid or hyperboloid of one sheet. Observed structures (see Fig. 10 of Salemme & Weatherford, 1981*a*) have more extensive interchain hydrogen bonding than is compatible with the geometrical requirements for regularly hydrogen-bonded configurations, and so in reality incorporate both regions composed of straight-helical chains, and chains of coiled-coil conformation in order to attain the necessary curvature required to close the structure. Note that, since the parallel coiled-coil configurations conform to superhelix axes that intersect the interchain hydrogen bonds (the broken line in (a); see also Fig. 3 of Salemme & Weatherford, 1981*a*), relatively little improvement in interchain hydrogen bonding is attained in parallel barrels composed of coiled-coil chains relative to structures composed of straight-helical polypeptide chains. In either case, the observed structures (see Fig. 10 of Salemme & Weatherford, 1981*a*) clearly manifest chain divergence at the barrel ends characteristic of the formation of a catenoid-like surface configuration.

Figure 5(d) shows the geometry of the antiparallel coiled-coil, which differs from the corresponding parallel arrangement in that twisting the antiparallel structure is achieved without the introduction of any deformative stresses into the interchain hydrogen bonds and results in double-strand helical structures whose hydrogen bonds lie tangent to a cylinder whose major axis (broken line) is the supercoil axis of the individual polypeptide chains (see Fig. 5 of Salemme & Weatherford, 1981*b*).

---

barrel composed of coiled-coil chains. Observed structures typically have more extensive interchain hydrogen bonding than is compatible with the twist required for closure. Consequently, they both depart from true cylindrical geometry and incorporate various conformational and hydrogen bonding defects resulting from the extensive twist of the polypeptide chains. (g) and (h) Triple-strand antiparallel variations that reflect the extensive conformational flexibility of antiparallel structures. (i) An idealized antiparallel, domed sheet composed of slightly twisted coiled-coils that obey a common (broken line) superhelix axis. Further discussion is given in the text.

As a consequence, isolated antiparallel double-strand structures can form very well-packed structural domains (Richards, 1977), which are relatively unstressed in the sense that optimal side-chain packing is achieved without the introduction of deformative stress into the interchain hydrogen bonds.

Figure 5(e) shows the isotropically stressed configuration of extended antiparallel sheets of rectangular plan. These share the basic geometrical characteristics of the related parallel rectangular sheets (Fig. 5(b)), but differ from them in the following respects. Owing to the potential variability of the interchain hydrogen-bond geometry in antiparallel structures (see Fig. 3 of Salemme & Weatherford, 1981*b*), the local chain conformations of such structures are to some extent dictated by requirements of favorable steric interactions among the sheet side-chain residues (see Fig. 6 of Salemme & Weatherford, 1981*b*). However, antiparallel structures possess considerable conformational flexibility within the limits dictated by side-chain steric interactions, so that they frequently exhibit spatial arrangements that reflect their more elastically deformable characteristics (see Figs 10 and 13 of Salemme & Weatherford, 1981*b*). This conformational flexibility is not present in parallel sheets, where there exists a preferred hydrogen-bond geometry that relatively defines the local polypeptide conformations best suited for the formation of an extended sheet of a given interchain twist (see Fig. 2 of Salemme & Weatherford, 1981*a*). As a consequence, the observed configurations of antiparallel sheets frequently reflect the more continuously deformable character that arises owing to this conformational flexibility and may, for example, result in the formation of sheets in which the edge chains take on a recognizable degree of coiled-coil character (see Fig. 16(c) of Salemme & Weatherford, 1981*b*).

Figure 5(f) shows the idealized geometry of the antiparallel staggered sheet forming a barrel structure. Owing to the unique geometrical behavior of the antiparallel coiled-coil conformations (Fig. 5(d)), such structures might potentially be composed wholly of coiled-coil chains. Nevertheless, both the model studies and examination of observed structures suggest that regularly, cyclically hydrogen-bonded structures are not readily formed from regular coiled-coil chains, since (as was the case for parallel barrels) the requirements for the formation of regular and extended interchain hydrogen bonding are geometrically incompatible with the attainment of a structure of suitably small cylindrical radius. The observed structures manifest this effect in their incorporation of hydrogen bonding and conformational defects (see below), which suggests that barrel closure requires the chains to be more twisted than is compatible with the maintenance of regular interchain hydrogen bonding. However, the fact that antiparallel barrels generally incorporate fewer strands than parallel barrels is indicative of the relatively large extent of twist that can be accommodated in the antiparallel coiled-coil conformations, although these antiparallel barrel structures again manifest the divergent character of the catenoid structure at the barrel ends (see Fig. 15 of Salemme & Weatherford, 1981*b*).

Figure 5(g) illustrates β-bulge formation (Richardson *et al.*, 1978), which generally occurs when an antiparallel sheet structure becomes twisted to a greater extent than is compatible with the maintenance of the overall interchain hydrogen bonding. The fact that such arrangements, which are extremely common in

strongly twisted antiparallel structures (e.g. see Figs 13 and 15 of Salemme & Weatherford, 1981*b*), do not generally occur in parallel sheets reflects the inherent conformational flexibility of antiparallel coiled-coil conformations, which may readily undergo entensive twisting (see Fig. 5 of Salemme & Weatherford, 1981*b*) concomitant with variations in the interchain hydrogen-bonding geometry and local chain conformations (see Fig. 10(c) of Salemme & Weatherford, 1981*b*).

Figure 5(h) shows a less twisted helicoid triple-strand antiparallel sheet, which reflects an overall equilibration of the forces causing the chains to twist and the optimal preservation of the interchain hydrogen bonds. Again, the facility with which such structures may be formed in antiparallel structures is related to the conformational flexibility of antiparallel sheet arrangements (see Fig. 11 of Salemme & Weatherford, 1981*b*). In a sense, the bulge arrangement shown in Figure 5(g) can be viewed as a highly twisted variation of the helicoid surface shown in (h); i.e. whereas the helicoid surface represents a stress equilibrium between the twist and packing forces and the interchain hydrogen bonding requirements throughout the sheet, bulge formation represents the situation in which the twist and packing forces in a strand pair dominate, so necessitating the formation of a local conformational defect in the third strand of the model shown in (g).

Figure 5(i) illustrates a "domed" antiparallel β-sheet, which is effectively composed of chains having slight coiled-coiled character. Note that the formation of such structures depends on the fact that antiparallel coiled-coil conformations form super-helices whose major axes lie outside the structure (e.g. the broken line). This is not a property of the parallel coiled-coils (Fig. 5(a)), which consequently do not form such arrangements having a net apparent curvature as a result of the slight coiling of the antiparallel chains on the "super-barrel" surface. It is of interest to compare the properties of the domed sheet with that of the hyperbolic paraboloid antiparallel sheet shown in Figure 5(e). In the case of the latter structure composed of straight helical chains, the assumed spatial configuration reflects an equilibrium between the requirements of interchain hydrogen-bond formation and chain twisting in a situation where the packing environment on both sides of the sheet is equivalent. Such arrangements are therefore typically found in the interior of protein structures. Sheet doming, in contrast, reflects a situation in which the polypeptide chains attain more or less continuously varying coiled-coil conformations which, nevertheless, preserve reasonably good interchain hydrogen bonding (owing to both the inherent conformational flexibility and hydrogen-bonding characteristics of antiparallel coiled-coils (see Fig. 5 of Salemme & Weatherford, 1981*b*)) in response to differing environments on opposite sides of the sheet. Therefore, domed sheets, which typically occur on exterior protein surfaces (see Fig. 13 of Salemme & Weatherford, 1981*b*) are seen to reflect the elastic deformation of the sheet in order to attain an isotropically stressed surface configuration in which there effectively exists a surface tension or pressure differential across the plane of the sheet. In other words, these sheets are elastically deformed, insofar as is consistent with the geometrical requirements for preservation of the interchain hydrogen bonds, to form surfaces of quasi-spherical curvature. They might consequently be viewed simply as soap bubbles whose

deviations from uniform spherical curvature reflect geometrical limitations inherent in the actual interactions formed between the polypeptide chains.

(c) *Conformational irregularity in protein β-sheets*

It has been shown here that the geometrical properties of twisted β-sheets can be understood in terms of a generalized model that approximates them as deformable lattice structures, whose final configuration reflects the interaction of both local conformational effects associated with the preservation of interchain hydrogen

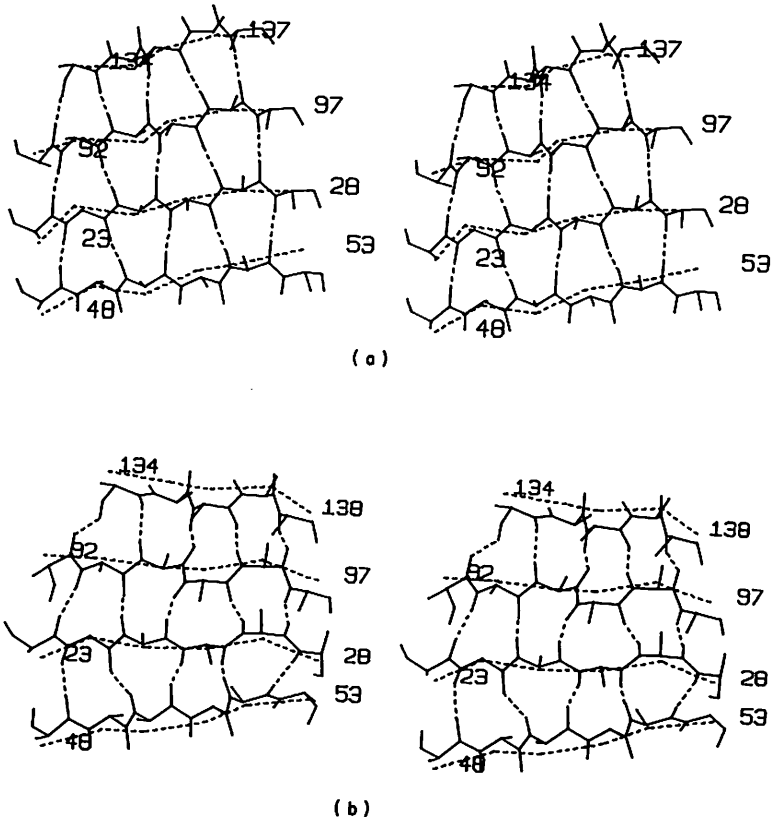

FIG. 6. (a) A least-squares fit of a conformationally regular crossing model ($\phi = -114°$, $\psi = 124°$, average NHO bond length 2·83Å with a standard deviation of 0·15Å) with the 4 most regular strands of the parallel β-sheet in lactate dehydrogenase. The average superposition error for corresponding model and observed α-carbon positions is 0·60Å. (b) A least-squares fit of a generated model having regular polypeptide geometry, observed ϕ, ψ values, and least-squares optimized interchain hydrogen bonds, fit to the observed structure. This model has more highly distorted interchain hydrogen bonds (average length 3·08Å with a standard deviation of 0·48Å) and Cβ packing interactions than the regular model. The average generated model *versus* observed structure α-carbon superposition error is 0·91Å. Although this fit may be improved by fitting individual generated chains to each of the observed chains, the hydrogen bonds of the resulting model structure become correspondingly worse than those of the hydrogen-bond optimized structure. As described previously, the extended parallel sheet is among the most conformationally restricted structures (see Fig. 2 of Salemme & Weatherford, 1981*a*) owing to geometrical requirements associated with hydrogen bond preservation in the twisted structures.

bonding, and global effects related to isotropic stress distribution within the sheet as a whole. Nevertheless, few observed structures exhibit the conformational regularity inherent in the generated model structures. The origin of this effect lies in the actual non-equivalence of the side-chain packing interactions in extended β-sheets. For example, Figure 6 shows least-squares fits of both a conformationally regular model structure and generated model structure to the observed α-carbon co-ordinates of the four most regular chains of the parallel sheet in lactate dehydrogenase (Chandrasekhar *et al.*, 1973). The generated model structure was produced by least-squares superposition of interchain hydrogen-bonding groups between chains of regular polypeptide geometry (to avoid effects that might arise from geometrical irregularity in the observed co-ordinates) incorporating the observed ϕ, ψ values. While both models produce acceptable fits (average errors of 0·60Å and 0·91Å for the conformationally regular and generated model *versus* observed structure, respectively), it is readily seen from Figure 6 that the hydrogen bonding of the generated model is more distorted than for the conformationally regular model. This is most probably a consequence of the non-equivalence of the packing interactions among the actual residues in the sheet, which will generally have different packing volumes and/or interactions with other structural elements of the protein. The side-chain packing lattice is locally perturbed as a consequence of these non-equivalent side-chain interactions, and results in local displacements in the positions of the Cβ atoms relative to their positions in the idealized structure. These local displacements in Cβ induce a torsional moment about the polypeptide chains axis that is accommodated by local rotations of the peptide bond planes which, in turn, introduce further localized deformations into the interchain hydrogen bonds. The observed, apparently conformationally irregular, structures can consequently be seen to reflect the effects of locally induced, conformational perturbations upon an underlying regular, isotropically stressed, lattice structure.

As is well documented in the literature (Ooi *et al.*, 1978), the introduction of localized peptide bond rotations, particularly in polypeptide chains of extended conformation, introduces relatively small displacements at Cα, owing to the near parallelism of the $C\alpha(i)-C'(i)$ and $N(i+1)-C\alpha(i+1)$ peptide bonds. Indeed, it is clear that it is this geometrical feature of the polypeptide chain structure that allows their ready approximation as conformationally regular structures whose properties are dictated by extended, rather than localized, interchain hydrogen-bonded interactions.

(d) *The invariant twist in β-sheets*

Chothia (1973), who first noted the invariant right-handed twist sense in β-sheets, principally attributed the effect to entropic factors; i.e. β-sheets were assumed to be right-twisted, since there exists a greater number of sterically allowed polypeptide conformations lying to the right of the $n = 2$ line on the ϕ, ψ plot (Dickerson & Geis, 1969). However, it is evident from the accompanying studies of the conformational restrictions associated with the preservation of interchain hydrogen bonding that this numerical preponderance of sterically accessible left-helical conformations has little to do with the observed preferred

β-sheet twist, since the excess left-helical conformations correspond to collagen-like conformations that simply cannot be arranged to make β-sheet structures. The work presented here has assumed that the invariant chiral twist is a result of the tendency of extended chains to form locally left-twisted helices, as is indeed consistent with the frequent occurrence of right-twisted supercoiled character both in β-sheets and a variety of supersecondary structural domains (Richardson, 1976; Sternberg & Thornton, 1976,1977; Weber & Salemme, 1980). However, it was recently noted that such effects could also arise owing to systematic chiral deformations of the inter-residue peptide bonds (Weatherford & Salemme, 1979). This was suggested on the basis of theoretical and X-ray studies, which showed that variances of the peptide bond from planarity were accompanied by the introduction of some degree of tetrahedral (sp^3) character into the peptide nitrogen atom (Ramachandran *et al.*, 1973; Renugopalakrishnan & Rein, 1976; Ramachandran & Kolaskar, 1973). This in turn results in the formation of a chiral center at the peptide nitrogen, so that peptides having opposite senses of tetrahedral deformation (e.g. see Fig. 6 of Weatherford & Salemme, 1979) are diasteriometrically related, and so might reasonably be expected to differ in energy. Subsequently, it was shown that deformations that give positive variations in the C′–N torsional bond angle (ω) improve the interchain hydrogen bonding in right-twisted β-sheets owing to the accompanying tetrahedral distortion of the amide nitrogen. The tendency for ω to assume a positive deviation from planarity has been observed in the 1·2 Å resolution structure of rubredoxin, the only protein that has thus far been refined by methods that make no implicit assumptions about the structure's geometry (Watenpaugh *et al.*, 1979). Nevertheless, it appears likely that this systematic distortion of the peptide plane planarity may be a result, rather than a cause of twisting in the sheets. This is suggested by comparison of the potential functions governing deformation of the amide peptide plane (Ramachandran, 1974; Ramachandran *et al.*, 1973; Renugopalakrishnan & Rein, 1976; Ramachandran & Kolaskar, 1973) with that governing deformation of the interchain hydrogen bonding (Hagler *et al.*, 1974). As described above, both the regular twisting of extended sheets, and particularly the introduction of local deformations arising as a consequence of non-equivalent side-chain packing interactions, frequently induce large distortions in the interchain hydrogen bonds. In this case, it is probable that the total potential energy of the hydrogen-bonded interaction may be minimized by a compensating deformation in the planarity of the amide peptide bonds. The fact that both the observed conformational (ϕ, ψ) and peptide tortional (ω) values exhibit only a statistical tendency to be locally left-twisted in either case reflect the effects of local packing perturbations on underlying regularly twisted lattice structure.

3. Conclusion

The folding of an extended polypeptide chain to ultimately form a unique three-dimensional configuration is generally assumed to reflect the co-operative minimization of the forces governing the interactions both among various parts of the structure and the surrounding solvent. The results presented here have shown

that the geometrical properties of twisted β-sheets in proteins can be understood as consequences of their inherent conformational properties and concomitant requirements for the optimal preservation of interchain hydrogen bonding. The observation of importance is that the spatial configurations of twisted β-sheets generally reflect a compromise between the opposing forces that cause the individual chains to twist, and the conformational and geometrical constraints associated with the preservation of interchain hydrogen bonding, which tend to resist the introduction of twist into the sheets. As a consequence, these structures assume the well-known spatial arrangements characteristic of isotropically stressed surfaces. The presence of counteracting stresses in sheets, together with their frequent formation of anticlastically curved surfaces, suggest that twisted β-sheets are relatively rigid structures. Indeed, this is the basic reason why such surfaces find extensive application in architectural practice (Otto, 1969). Nevertheless, it is evident that various β-sheets differ in the relative contributions of the forces that cause them to exhibit a particular spatial configuration. The configurations of extended parallel sheets, for example, appear to be mainly dictated by conformational restrictions associated with interchain hydrogen-bond preservation, whereas the more elastically deformable extended antiparallel sheets can frequently exhibit spatial configurations that reflect more variable responses to very generalized extended packing forces. Indeed, the double-strand antiparallel coiled-coil configuration would appear to represent an extreme case of an intrinsically highly flexible structure whose observed arrangement depends almost wholly on the attainment of intimate side-chain packing interactions.

Perhaps the most fundamental observation to emerge from this study, however, is that these structures clearly manifest mechanical effects that are propagated, and hence co-operative, throughout the entire structure. This suggests that these long-range co-operative interactions may reflect themselves in the thermally induced dynamic behavior of proteins, and additionally provide highly co-operative pathways by which proteins might fold to their final tertiary configuration.

This research was supported by grants from the National Institutes of Health (GM21534 and GM25664), the University of Arizona Computer Center, and a Dreyfus Teacher-Scholar Grant (to F. R. S.).

REFERENCES

Boys, C. V. (1959). In *Soap Bubbles*, pp. 55–58, Dover, Inc., New York.

Chandrasekhar, K., McPherson, A., Adams, M. J. & Rossmann, M. G. (1973). *J. Mol. Biol.* **76**, 503–528.

Chothia, C. (1973). *J. Mol. Biol.* **75**, 295–302.

Dickerson, R. E. & Geis, I. (1969). In *The Structure and Action of Proteins*, pp. 24–43, W. A. Benjamin, Menlo Park.

Gellert, W., Kustner, H., Hellwich, M. & Kastner, H. (1977). In *VNR Concise Encyclopedia of Mathematics*, pp. 544–547, Van Nostrand, New York.

Hagler, A. T., Lifson, S. & Huler, E. (1974). In *Peptides, Polypeptides and Proteins* (Blout, E. R., Bovey, F. A., Goodman, M. & Lotan, N., eds), pp. 35–48, Wiley Interscience, New York.

Ooi, T., Nishikawa, K., Oobatake, M. & Scheraga, H. A. (1978). *Biochim. Biophys. Acta*, **536**, 390–406.

Otto, F. (1969). *Tensile Structures*, MIT Press, Cambridge, Mass.
Ramachandran, G. N. (1974). In *Peptides, Polypeptides and Proteins* (Blout, E. R., Bovey, F. A., Goodman, M. & Lotan, N., eds), pp. 14–34, Wiley Interscience, New York.
Ramachandran, G. N. & Kolaskar, A. S. (1973). *Biochim. Biophys. Acta*, **303**, 385–388.
Ramachandran, G. N., Lakshminarayan, A. V. & Kolaskar, A. S. (1973). *Biochim. Biophys. Acta*, **303**, 8–13.
Renugopalakrishnan, V. & Rein, R. (1976). *Biochim. Biophys. Acta*, **434**, 164–168.
Richards, F. M. (1977). *Annu. Rev. Biophys. Bioeng.* **6**, 151–176.
Richardson, J. S. (1976). *Proc. Nat. Acad. Sci., U.S.A.* **73**, 2619–2623.
Richardson, J. S. (1977). *Nature (London)*, **268**, 495–500.
Richardson, J. S., Getzoff, E. D. & Richardson, D. C. (1978). *Proc. Nat. Acad. Sci., U.S.A.* **75**, 2574–2578.
Salemme, F. R. & Weatherford, D. W. (1981*a*). *J. Mol. Biol.* **146**, 101–117.
Salemme, F. R. & Weatherford, D. W. (1981*b*). *J. Mol. Biol.* **146**, 119–141.
Sternberg, M. J. E. & Thornton, J. M. (1976). *J. Mol. Biol.* **105**, 367–382.
Sternberg, M. J. E. & Thornton, J. M. (1977). *J. Mol. Biol.* **110**, 269–283.
Watenpaugh, K. D., Siecker, L. C. & Jensen, L. H. (1979). *J. Mol. Biol.* **131**, 509–522.
Weatherford, D. W. & Salemme, F. R. (1979). *Proc. Nat. Acad. Sci., U.S.A.* **76**, 19–23.
Weber, P. C. & Salemme, F. R. (1980). *Nature (London)*, **287**, 82–84.